European Journal of Chemistry

View Journal Online
View Article Online

Hydrogen bonding framework in imidazole derivatives: Crystal structure and Hirshfeld surface analysis

Praveen Singh [1], Ranjeet Kumar [2] and Ashish Kumar Tewari [1,*]

[1] *Department of Chemistry, Centre of Advance Studies, Institute of Science, Banaras Hindu University, Varanasi 221005, India*
prs281986@gmail.com (P.S.), ashishtewarichem@gmail.com (A.K.T.)
[2] *Department of Chemistry, Chaudhary Mahadeo Prasad Degree College, Allahabad, 211002, India*
bhuranjeet@gmail.com (R.K.)

* *Corresponding author at: Department of Chemistry, Centre of Advance Studies, Institute of Science, Banaras Hindu University, Varanasi 221005, India.*
e-mail: ashishtewarichem@gmail.com (A.K. Tewari).

RESEARCH ARTICLE

10.5155/eurjchem.11.1.50-59.1945

Received: 12 December 2019
Received in revised form: 19 January 2020
Accepted: 28 January 2020
Published online: 31 March 2020
Printed: 31 March 2020

KEYWORDS

Synthesis
Crystal structure
Hydrogen bonding
Imidazole derivative
Hirshfeld surface analysis
Intermolecular interactions

ABSTRACT

A series of imidazole derivatives (1-3) were synthesized with three component reaction among benzil, ammonium acetate and formaldehyde/aromatic aldehyde at 110 °C without a catalyst and solvent. These synthesized imidazole derivatives have shown intermolecular hydrogen bonding such as N-H···N and O-H···N. The imidazole 1 and 2 exhibited N-H···N intermolecular hydrogen bonding while imidazole 3 exhibited O-H···N intermolecular hydrogen bonding. The hydrogen bonds in imidazoles were studied by X-ray crystallography and Hirshfeld Surface Analysis at d_{norm} surface which show the visible red spots, indicated for hydrogen bonds. Further, Hirshfeld surface analysis also shows the percentage of all intermolecular interactions.

Cite this: *Eur. J. Chem.* **2020**, *11(1)*, 50-59 **Journal website**: www.eurjchem.com

1. Introduction

The imidazole derivatives have attracted more attention during recent years due to their application in biological activities. The imidazole derivative are known to show as an anti-inflammatory [1,2], antibacterial [3], antifungal [4], anthelmintic [5,6], analgesic [7], antiviral [8], antitubercular [9], anticancer [10] activities and COX-2/LOX inhibitor [11]. They are also known as melanocortin-4-receptor (MC4-R) antagonists [12], inhibitors of P38MAP kinase [13], herbicides [14] and plant growth regulators [15]. Besides their biological and pharmacological activities they also act as dyestuff catalysts, polymerizing agent [16,17] and also photo sensitizers in photography [18,19]. The potency and wide applicability of the imidazole pharmacophore can be attributed to its hydrogen bond donor-acceptor capability [20]. Hydrogen bonding is particularly important from the biological point of view, because of its participation in several biological processes such as: the stabilization of the double helix of DNA [21], enzyme-substrate interactions [22], recognition among proteins [23] and drug-acceptor interactions [24]. Further, hydrogen bonding is the most important in the design of self-assembled organic molecules [25-29]. The strong hydrogen bonds, such as O/N–H···O/N have been recognized as the key factor for providing the requisite robustness and architectures of supramolecular synthons [30-33]. Further, hydrogen bonding in imidazole such as N–H···N [34] employed in new classes of electronic materials, ferroelectric, relaxer materials with desired dielectric properties and exhibited ionic conductivity due to proton transfer [35-40].

Therefore, we synthesized the diaryl as well as triaryl substituted imidazole for studies of intermolecular hydrogen bonding such as O/N–H···O/N between imidazole derivative in solid state.These hydrogen bonding occurred because of strong correlation between the distributions of the N-H···O and N-H···N due to advantages offered by the basicity of the nitrogen atom and the exalted acidity by sp^2 hybridization at the nitrogen atom and hydroxyl group, allowing stable hydrogen bond donation and acceptance. This was present in the crystal structure, even with sterically crowded molecular environments [41,42].

2. Experimental

2.1. Instrumentations

ISSN 2153-2249 (Print) / ISSN 2153-2257 (Online)
http://dx.doi.org/10.5155/eurjchem.11.1.50-59.1945

Table 1. Crystallographic details of compounds **1**, **2** and **3**.

Compounds	1	2	3
Empirical formula	$C_{15}H_{12}N_2$	$C_{22}H_{18}N_2O$	$C_{21}H_{16}N_2O$
Formula weight	220.27	326.38	312.36
Temperature (K)	293	293	293
Crystal system	Monoclinic	Triclinic	Triclinic
Space group	$P2_{1/c}$	P-1	P-1
a (Å)	11.161(5)	8.9772(3)	10.5451(9)
b (Å)	9.263(5)	12.0646(5)	12.4531(9)
c (Å)	11.794(5)	33.6434(14)	13.8175(10)
α (°)	90.00	100.015(4)	68.757(7)
β (°)	93.572(5)	95.733(3)	86.626(7)
γ (°)	90.00	91.590(3)	85.711(7)
μ (mm^{-1})	0.07	0.08	0.08
Cell volume, V ($Å^3$)	1216.95	3566.5(2)	1685.5(2)
D_{calc} (mg/m^3)	1.202	1.216	1.231
F (000)	464	1376.0	656
Z	4	8	4
Theta range (°)	3.28-29.21	3.30-26.70	3.02-29.12
2Θ range for data collection (°)	10-50	01-50	5.5-50
Goodness-of-fit on F^2	1.022	1.05	0.988
h	-15, 15	-10, 11	-10,14
k	-12, 12	-15, 12	-15, 15
l	-16, 16	-39, 42	-18, 17
R%	4.71	9.0	6.38
CCDC No	972006	972017	972011

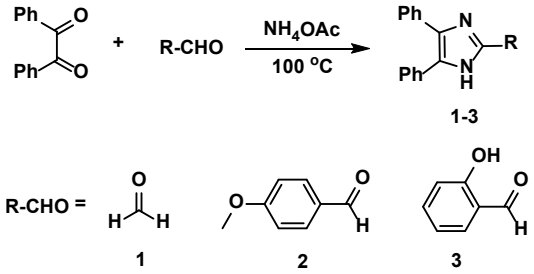

Scheme 1. Synthesis of imidazole derivatives.

^1H and ^{13}C NMR spectra were recorded on JEOL AL300 FT-NMR spectrometer (300 MHz). TMS was used as internal reference, and chemical shift values were expressed in δ ppm units. Elemental characterization was done using CHNS 2400 Perkin Elmer (PE 2400 Series II CHNS/O Analyzer, Shelton, USA). Melting points were taken in open glass capillary using Veego VMP-CM melting point apparatus and are uncorrected.

2.2. Synthesis of compounds (1-3)

All reactions were performed in ordinary conditions at ambient temperature, and reagents were used without further purification. Imidazole derivative are synthesized by three-component reaction between benzil, ammonium acetate and formaldehyde/aromatic aldehyde at 110 °C without a catalyst, in solvent free condition. The reaction is completed within 5 minutes having excellent yield. The simple work-up procedure, mild reaction conditions and good yields make this methodology eco-friendly (Scheme 1).

4,5-Diphenyl-1H-imidazole (**1**): M.p.: 228-230°C. Yield: 0.60 g (88%). ^1H NMR (300 MHz, $CDCl_3$, δ, ppm): 7.25-7.31 (m, 4H, Ar-H), 7.36-7.39 (d, 1H, Ar-H), 7.47-7.52 (m, 4H, Ar-H), 7.62-7.68 (m, 2H, Ar-H), 7.94-7.96 (d, 1H, N-H). ^{13}C NMR (75 MHz, $CDCl_3$, δ, ppm): 126.4, 126.45, 127.20, 127.85, 128.07, 128.16, 128.43, 128.58, 128.65, 128.73, 128.98, 129.63, 129.86, 130.34, 130.93, 134.90, 136.47, 140.40. Anal. calcd. for $C_{15}H_{12}N_2$: C, 81.79, H, 5.49; N, 12.72. Found: C, 82.79, H, 5.40; N, 11.81%.

2-(4-Methoxyphenyl)-4,5-diphenyl-1H-imidazole (**2**): M.p.: 220-223 °C. Yield: 0.60 g (85%). ^1H NMR (300 MHz, $CDCl_3$, δ, ppm): 3.86 (s, 3H, OCH_3), 6.96-6.99 (d, 3H, Ar-H), 7.30-7.36 (m, 6H, Ar-H), 7.55 (s, 5H, Ar-H), 7.83-7.85 (d, 1H, NH). ^{13}C NMR (75 MHz, $CDCl_3$, δ, ppm): 55.6, 111.5, 118.9, 120.6,126.4, 127.1, 127.6, 128.2, 128.9, 129.8, 131.2, 135.3, 136.4, 143.2, 156.0. Anal.calcd. for $C_{22}H_{18}N_2O$: C, 80.96, H, 5.56, N, 8.58. Found: C, 81.10, H, 5.28, N, 8.39%.

2-(4,5-Diphenyl-1H-imidazol-2-yl)phenol (**3**): M.p.: 203-207 °C. Yield: 0.55 g (82%). ^1H NMR (300 MHz, DMSO-d_6, δ, ppm): 5.95 (s, 1H, OH), 6.79-6.86 (m, 3H, Ar-H), 7.06-7.11 (m, 2H, Ar-H), 7.45-7.58 (m, 8H, Ar-H), 7.68-7.71 (d, 1H, Ar-H), 10.05 (s, 1H, NH). ^{13}C NMR (75 MHz, DMSO-d_6, δ, ppm): 52.6, 115.3, 118.9, 127.0, 127.6 128.2, 128.5, 129.1, 131.3, 134.6, 155.1, 165.3. Anal. calcd. for $C_{21}H_{16}N_2O$: C, 80.75, H, 5.16, N, 8.97. Found: C, 81.02, H, 5.32, N, 9.10%.

2.3. X-ray crystallography

Single-crystal X-ray data, space groups, unit cell dimensions, and intensity data for compounds **1**, **2** and **3** were collected with an Oxford Diffraction X-calibur CCD diffractometer using graphite monochromated MoKα radiation (λ = 0.71073 Å). The structures were determined by direct methods using SHELXS-97 and refined on F^2 by a full-matrix least-squares technique using SHELXL-97 [43]. Non-hydrogen atoms were refined anisotropically, and hydrogen atoms were geometrically fixed with thermal parameters equivalent to 1.2 times that of the atom to which they are bonded. Molecular diagrams (Figure 1) for all compounds were prepared using ORTEP [44] and the packing diagrams were generated using Mercury version 3.1 [45]. PLATON [46] was used for the analysis of bond lengths, bond angles, and other geometrical parameters. Crystallographic details of compounds **1**, **2** and **3** have been summarized in Table 1.

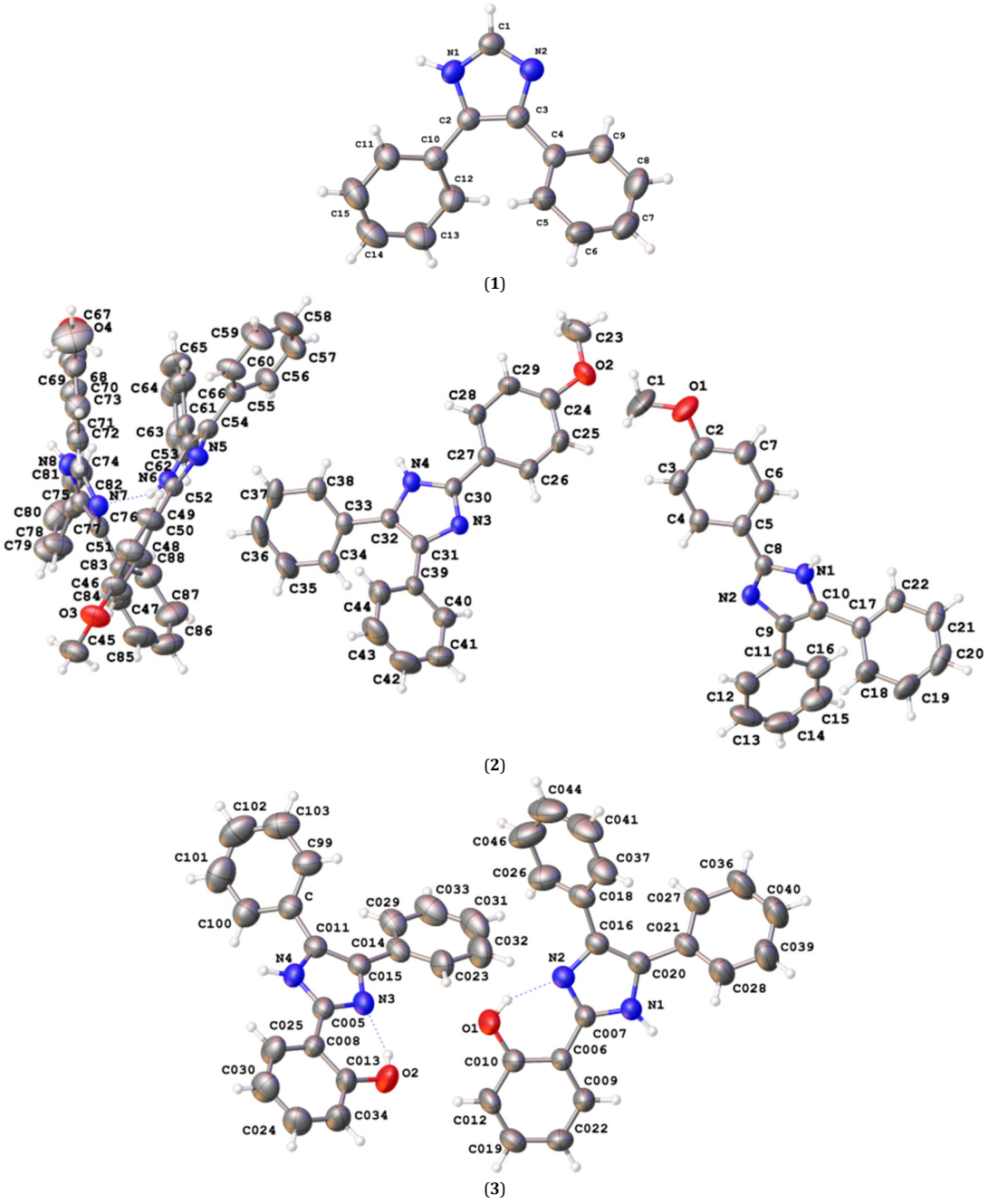

Figure 1. Molecular structure of compound **1**, **2** and **3**.

Compound 1: An X-ray diffracted quality crystal of compound **1** was crystallized in a mixture of ethyl acetate by slow evaporation at room temperature.

Compound 2: An X-ray diffracted quality crystal of compound **2** was crystallized in a mixture of chloroform and methanol (1:1) by slow evaporation at room temperature.

Compound 3: An x-ray diffraction quality crystal of compound **3** was grown from slow evaporation of ethyl acetate at room temperature.

2.4. Hirshfeld surface analysis

Hirshfeld surfaces provide a three-dimensional picture for exploring packing modes and close contacts in a crystal, and these contacts can be summarized in a two-dimensional (2D) fingerprint plot offered considerable promise for exploring packing modes and intermolecular interactions in molecular crystals. Hirshfeld surface also reflects the interplay between different atoms and intermolecular contacts in a crystal. Calculations were performed using the Crystal Explorer package [47].

3. Result and discussion

3.1. Crystallography details

In this section, we shall discuss about crystallographic details of compounds **1**-**3** particularly for studies of intermolecular N-H···N and O-H···N hydrogen bonding in imidazole derivatives that stabilized the geometry of molecules in 3D-space and generated a sheet like structure.

Table 2. Weak inter and intramolecular interactions in crystal structure of imidazole **1**, **2**, and **3**.

Compound	X-H···A	A···H (Å)	X-A (Å)	∠X-H-A (°)
1	C1-H1···π (Centroids of phenyl ring)	2.700	3.497	139.03
	C12-H12···π (Centroids of phenyl ring)	3.503	4.158	129.60
	C8-H8···π (Centroids of imidazole ring)	2.761	3.605	151.30
	N1-H···π (Centroids of phenyl ring)	2.951	3.828	156.08
	N1-H···N2	1.940	2.868	170(2)
	C11-H11···N2	2.991	3.655	129.65
2	C70-H70···π (Centroids of phenyl ring)	3.730	4.102	107.19
	N4-H2···π (Centroids of phenyl ring)	3.829	3.973	92.10
	N3-H90···N6	2.127	2.915	165.21
	C26-H26···N2	3.255	3.938	131.94
	N7-H···N2	2.09(6)	2.160	161(6)
3	C101-H101···π (Centroids of phenyl ring)	3.438	3.630	94.38
	C102-H102···π (Centroids of imidazole ring)	3.062	3.411	104.15
	C102-H102···π (Centroids of phenyl ring)	3.206	3.645	111.07
	C028-H028···π (Centroids of phenyl ring)	3.370	4.047	131.46
	C102-H102···N2	3.286	3.797	116.77
	N4-H···O1	1.86(3)	2.800	175(3)
	C025-H025···O1	2.581	3.455	156.97
	O1-H1···N2	1.779	2.526	150.68
	C5-H5···N3	2.707	3.524	146.96

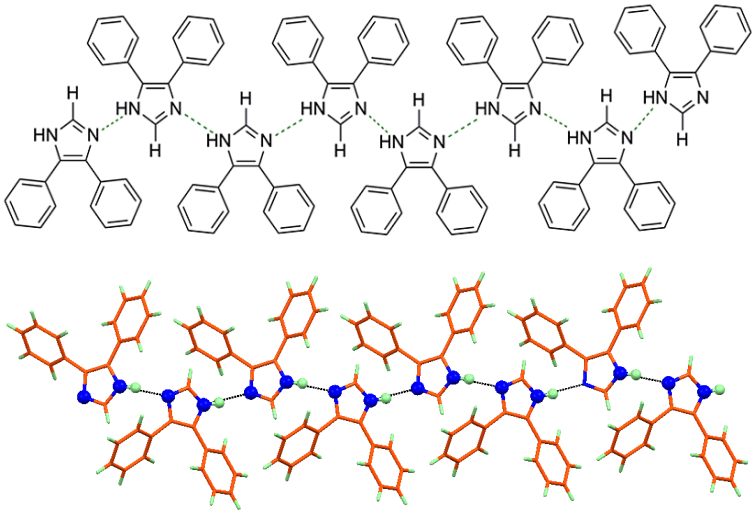

Figure 2. Views of the hydrogen bonding of compound **1**, hydrogen bonds are represented by black dotted lines. Carbon atoms are colored red, hydrogen atoms light green, and nitrogen atoms blue.

In spite of N-H···N and O-H···N hydrogen bonding there are another more interactions in packing of molecules that sustained and controlled through a combination of parallel displaced C-H···π, N-H···π, N-H···N and C-H···N interactions [48-55] (Table 2). Compound **1** crystallized in monoclinic crystal system with $P2_1/c$ space group having a, b and c values of 11.161(5), 9.263(5) and 11.794(5) Å, respectively. Compound **2** crystallized in triclinic crystal system with P-1 space group having a, b and c values of 8.9772(3), 12.0646(5) and 33.6434(14) Å, respectively. Compound **3** crystallized in triclinic crystal system with P-1 space group having a, b and c values of 10.5451(9), 12.4531(9) and 13.8175(10) Å, respectively. The other crystallography data such as cell parameters, space group are provided in Table 1.

The compound **1** possesses alternate N-H···N hydrogen bond between imidazole moieties of H and N2 of adjacent imidazole moieties having distances and angle are 1.94 Å (169.79°), forming sheet like structure in a zig-zag manner in opposite directions (Figure 2). Another more intermolecular interactions also found in packing of imidazole molecule that support the N-H···N hydrogen bonding (Figure 3). These interactions are C-H···π, N-H···π, and C-H···N. The C-H···π interactions occurred between phenyl protonwith centroids of imidazole nucleus and imidazole proton moieties with centroids of phenyl ring, because, π-electrons of aromatic moieties are known to act as H-bond acceptor and therefore, molecules of compound **1** have shown C-H···π networks between donor-acceptor systems. These C-H···π interactions play important role in stabilizing the overall intermolecular structural design.C-H···N interactions occurred between phenyl proton with nitrogen atom of imidazole nucleus.

The N-H···N intermolecular interactions in imidazole **2** also formed between imidazole moieties of H and N atom of adjacent imidazole moieties having distances and angle are 2.098 Å (160.30°), forming coordinated fashion that generated sheet like structure in same directions (Figure 4). The N-H···N hydrogen bonding in imidazole **2** is less than imidazole **1** because interaction distance in imidazole **2** is long compared to imidazole **1**. This difference in N-H···N hydrogen bonding occurred due to addition of anisole on imidazole **2** moieties which cause hindrance to increase interactions distances as well as packing occurred in same directions but in imidazole **1** packing found opposite directions.

Other intermolecular interactions like C-H···π, N-H···π, N-H···N and C-H···N, play an important role in sustaining the packing of molecules and stabilization of molecule in 3D-space (Figure 5). Among all intermolecular interactions N-H···N, C-H···π and N-H···π interactions are predominates. The C-H···π interactions occurred between phenyl hydrogen of H70 with phenyl rings, respectively. The C-H···N interactions occurred between phenyl hydrogen of H26 with N2 of imidazole nucleus.

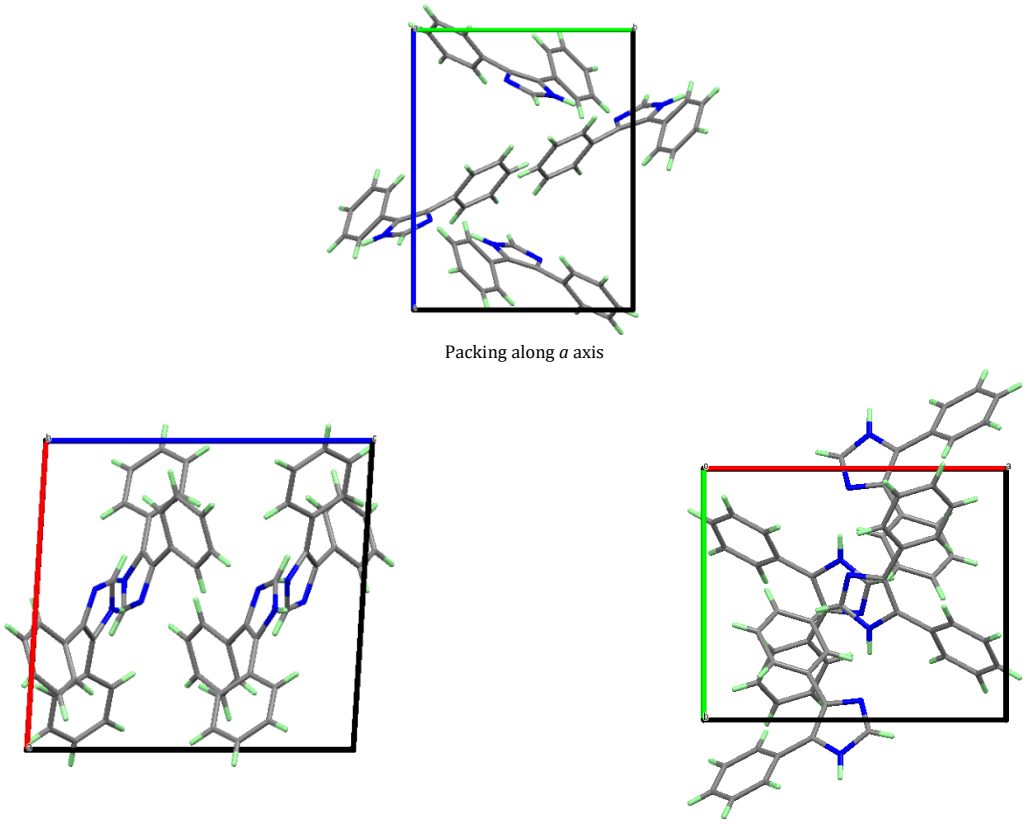

Packing along *a* axis

Packing along *b* axis

Packing along *c* axis

Figure 3. Packing of compound **1**, along *a*, *b*, and *c* axis.

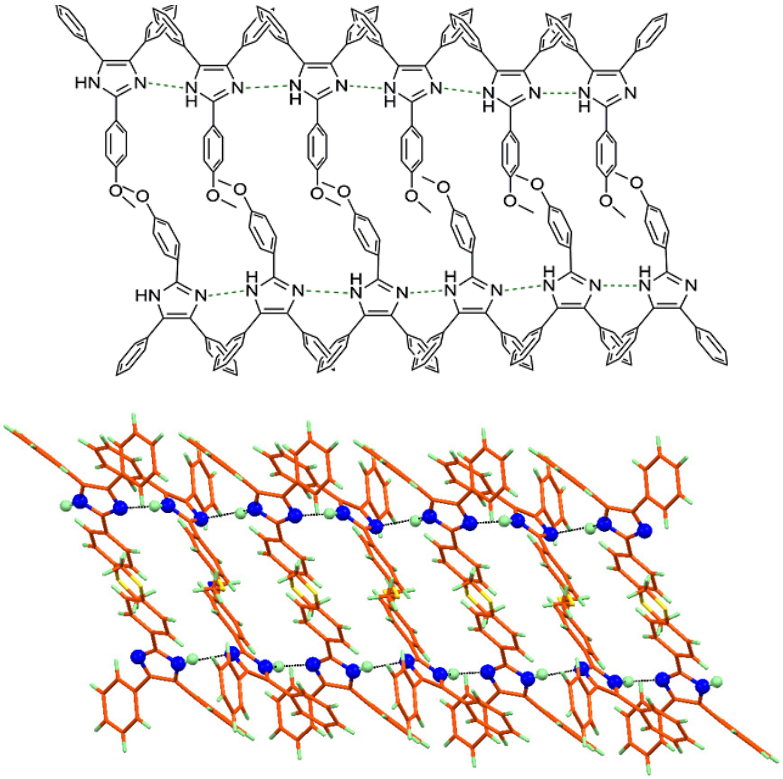

Figure 4. Views of the hydrogen bonding of compound **2**, hydrogen bonds are represented by black dotted lines. Carbon atoms are colored red, hydrogen atoms light green, oxygen atom yellow and nitrogen atoms blue.

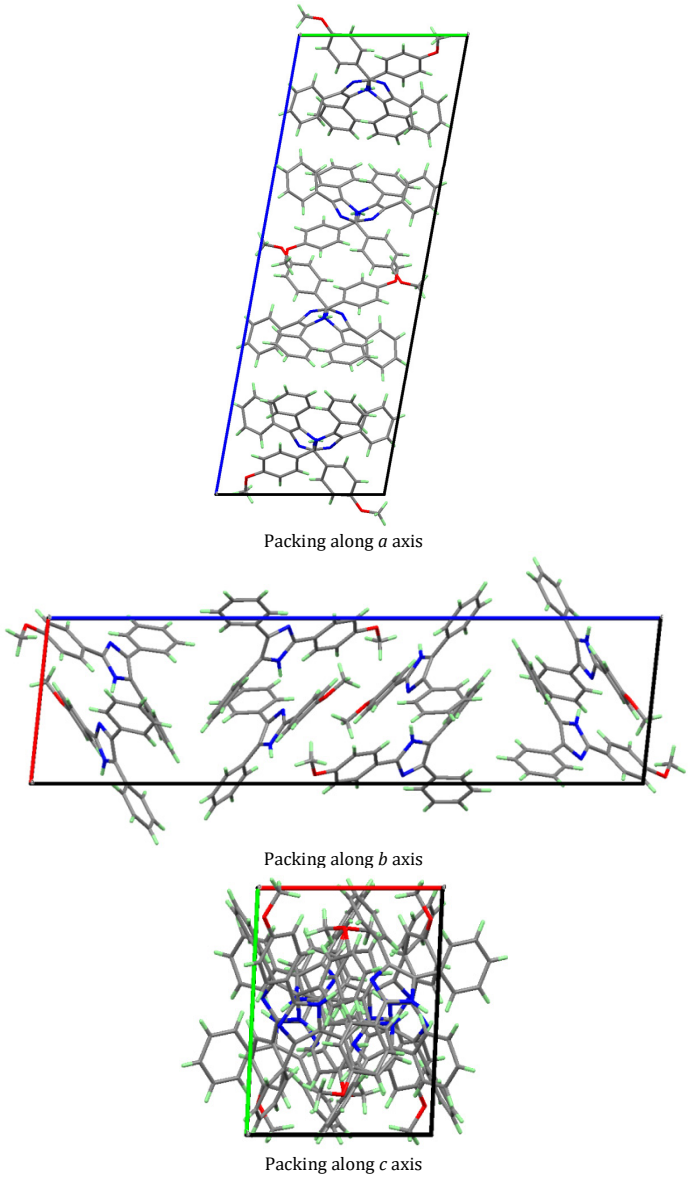

Figure 5. Packing of imidazole **2**, along *a*, *b*, and *c* axis.

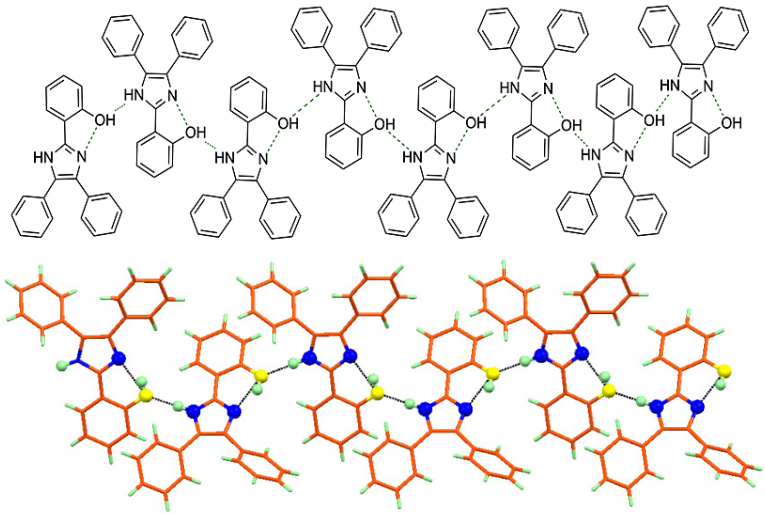

Figure 6. Views of the hydrogen bonding of compound **3**, hydrogen bonds are represented by black dotted lines. Carbon atoms are colored red, hydrogen atoms light green, oxygen atom yellow and nitrogen atoms blue.

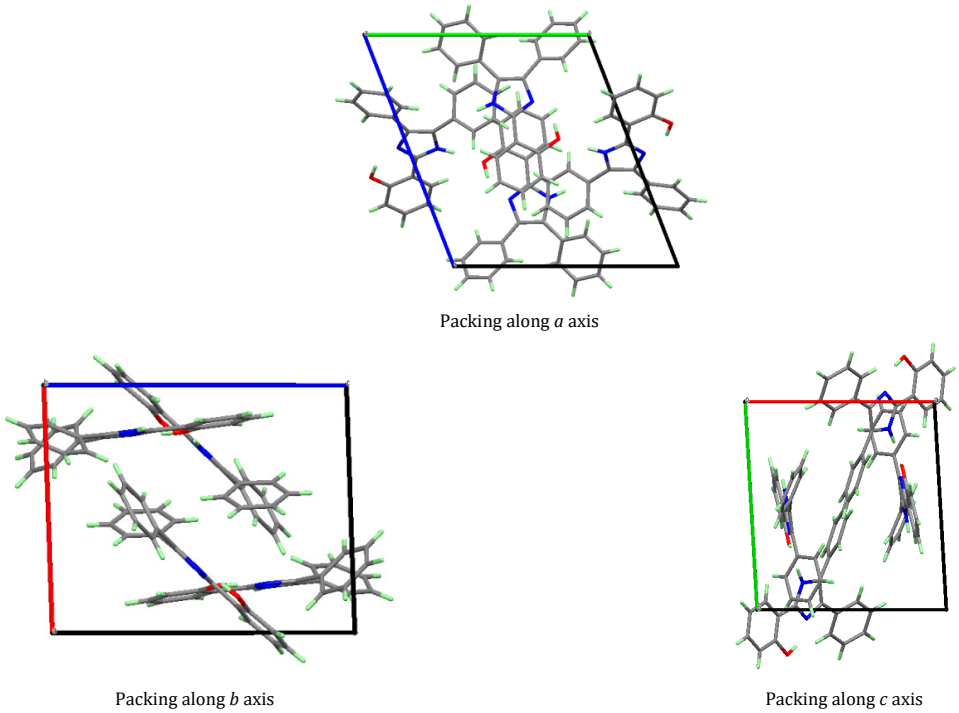

Figure 7. Packing of imidazole **3**, along *a*, *b*, and *c* axes.

In imidazole **3**, intermolecular N-H···O interaction occurred instead of N-H···N interactions because intramolecular O-H···N interaction found in imidazole **3** (Figure 6). The intramolecular N-H···O occurred due to presence of hydroxyl group in imidazole **3**. The imidazole **3** is also forming sheet like structure in a zig-zag manner in opposite directions due to intramolecular O-H···N and intermolecular N-H···Ohydrogen bond. The N-H···O hydrogen bond found between imidazole proton with hydroxyl oxygen atom of adjacent imidazole moieties having distance and angle are 1.86 Å (174.88°). In spite of N-H···O interaction another more interaction occurred like C-H···π, C-H···N, C-H···O, N-H···O and O-H···Ninteractions among which C-H···O, N-H···O and O-H···N interactions predominates for stabilization of packing and geometry of molecules in 3D-space (Figure 7).

The C-H···π interactions occurred between phenyl hydrogen of H101, H102, and H028 with centroids of phenyl ring respectively. The C-H···O interactions occurred between H025 with hydroxyl oxygen atom of adjacent imidazole moieties. The C-H···N interactions occurred between phenyl hydrogen of H5 and H102 with N2 and N3 of imidazole nucleus.

3.2. Hirshfeld surface analysis

In this section, the Hirshfeld surfaces of the titled compounds are illustrated, showing the surfaces that have been mapped over d_{norm} and two-dimensional fingerprint plots for showing percentages of intermolecular contact (Figure 8) [47]. The surfaces are shown as transparent to allow the visualization of the imidazole moieties in a similar orientation for all structures. The geometric parameters of d_{norm} surface which show the visible red spots indicated for hydrogen bonds and blue colour H···H, C···C and C···H contacts.

The most easily recognizable intermolecular interactions are of the type N–H···N, N–H···O and O-H···N seen in the Hirshfeld surfaces as red areas, and these are designated separately on the d_{norm} surfaces.The Hirshfeld surface of the imidazole **1** is illustrated in Figure 9 which shows surfaces that have been mapped over d_{norm}. The red color visible on the surfaces indicative of strong N–H···N interactions and the blue color points in the two-dimensional fingerprint plots are indicative of short contacts for the H···H, C···H and C···C interactions. The N–H···N interactions represent one of the closest contacts in the structures and can be viewed as the red spots on the d_{norm} surface, indicating the formation of intermolecular hydrogen bond.In imidazole **1**, the N–H···N intermolecular interactions appear as a sharp large spike in the two-dimensional fingerprint plots with d_i = 1.12 Å and d_e = 0.75 Å which comprises 11.4% of the total Hirshfeld surfaces.

The C···H interactions of total Hirshfeld surfaces of imidazole **1**, comprising 33.3% and reflected in the middle of the scattered points in the two-dimensional fingerprint plot (d_i = 1.6 Å and d_e = 1.08 Å). The H...H interactions comprise 54.5% to the total Hirshfeld surfaces and the two-dimensional fingerprint plot is (d_i = 1.20 and d_e = 1.15 Å) in the fingerprint plot. The π···π (C···C) interactions also have a relatively significant contribution to the total Hirshfeld surfaces of imidazole **1**, which comprises 0.9% as well as C···N contact in two dimensional finger print plot is comprises 0.3%.

The Hirshfeld surface of the imidazole **2** is illustrated in Figure 10, which shows surfaces that have been mapped over d_{norm}. In imidazole **2**, the N–H···N intermolecular interactions appear as a sharp large spike in the two-dimensional fingerprint plots with d_i = 1. 20 Å and d_e = 0.00 Å which comprises 5.5 % of the total Hirshfeld surfaces, which is visible red color on the surfaces indicative of strong N–H···N interactions. The C···H interactions of total Hirshfeld surfaces of compound **2**, comprising 25.7% in the two-dimensional fingerprint plot with d_i = 1.68 Å and d_e = 1.8 Å. The H···H interactions comprise 57.2% to the total Hirshfeld surfaces and the two-dimensional fingerprint plot is d_i = 1.10 and d_e = 1.10 Å in the fingerprint plot. The O···H interactions are comprise 4.9% represented by a spike having the d_i and d_e regions of 1.58 Å and 1.27 Å. The π···π (C···C) interactions also have a relatively significant contribution to the total Hirshfeld surfaces of imidazole **2**, which comprises 4.8% as well as C···N contact in two dimensional finger print plot is comprises 1.7%.

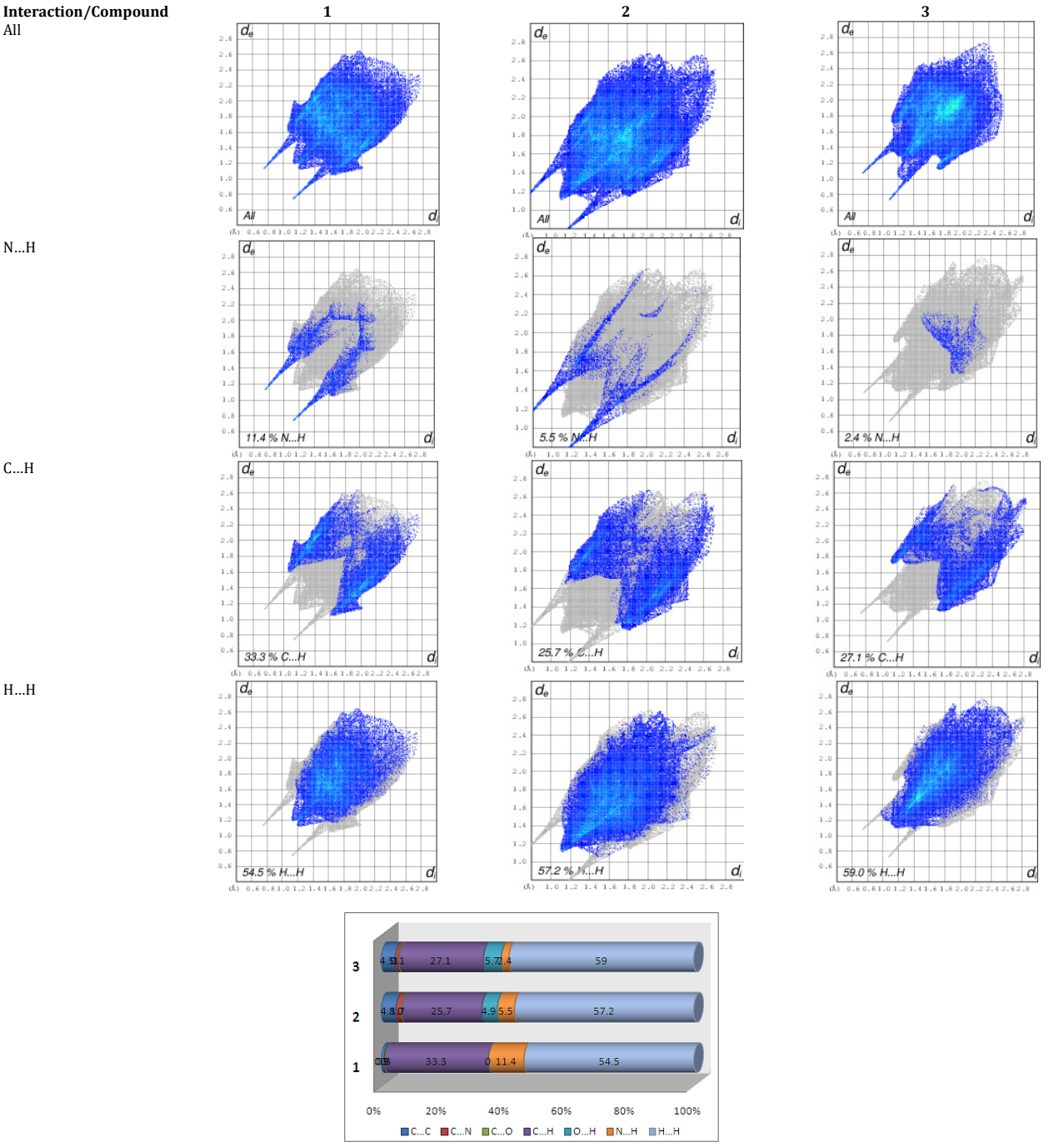

Figure 8. Hirshfeld surface of two-dimensional fingerprint plots for compounds (**1**, **2** and **3**).

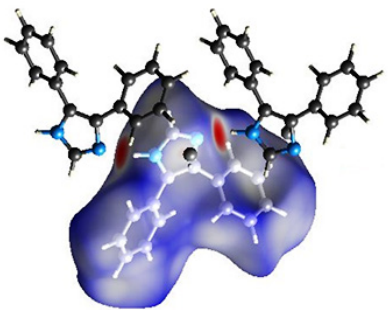

Figure 9. Hirshfeld surface of d_{norm} showing N–H···N intermolecular interactions indicated as red spot.

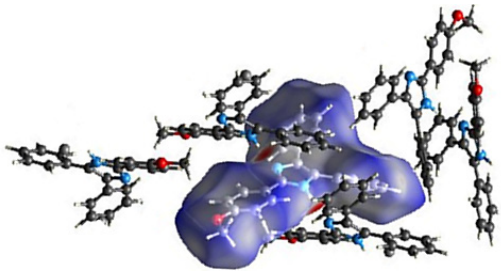

Figure 10. Hirshfeld surface of d_{norm} showing N–H···N intermolecular interactions indicated as red spot.

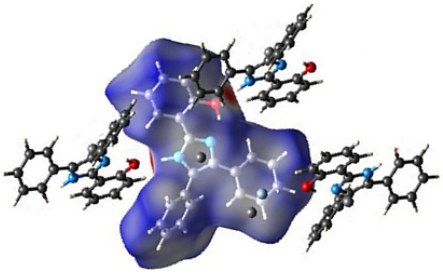

Figure 11. Hirshfeld surface of d_{norm} showing O–H···N intermolecular interactions indicated as red spot.

In imidazole **3**, dominant natures of the intermolecular O–H···N and N–H···O hydrogen bonds exhibited. This can be easily identified as red spot in d_{norm} surfaces (Figure 11). The H···N hydrogen bonds contribute 2.4% to the total Hirshfeld surfaces of the 2-D fingerprint plots, with d_i = 1.88 Å and d_e = 1.31 Å and the H···O hydrogen bonds contribute 5.7% to the total Hirshfeld surfaces and appear as a sharp large spike in region of the 2-D fingerprint plots, with d_i = 1.82 Å and d_e = 0.72 Å. The C···H interactions of total Hirshfeld surfaces of compound **3**, comprising 27.1% in the two-dimensional fingerprint plot (di = 1.71 Å and d_e = 1.91 Å). The H...H interactions comprise 59.0% to the total Hirshfeld surfaces and the two-dimensional fingerprint plot is d_i = 1.13 and d_e = 1.12 Å in the fingerprint plot. The C···O, C···C and N···C interactions comprise 0.1, 4.5 and 1.0 % of the total Hirshfeld surfaces, respectively.

4. Conclusion

X-ray crystallography studies shown that newly synthesized imidazole **1** and **2** exhibited N-H···N while imidazole **3** exhibited O-H···N intermolecular hydrogen bonding. The O-H···N intermolecular hydrogen bonding in imidazole **3** occurred due to hydroxyl group on phenyl ring.The hydrogen bonding in imidazole **1**, **2** and **3** also confirmed by Hirshfeld surface analysis as red spot in d_{norm} surfaces.

Acknowledgments

The author Praveen Singh and Ashish Kumar Tewari acknowledge University Grant Commission (Grant Sanction No. 37-54/2009) India for financial assistance of the work. Department of Chemistry, Banaras Hindu University, Varanasi, India is acknowledged for departmental facilities.

Supporting information

CCDC-972006, 972017, 972011 contains the supplementary crystallographic data for this paper. These data can be obtained free of charge via https://www.ccdc.cam.ac.uk/structures/, or by e-mailing data_request@ccdc.cam.ac.uk, or by contacting The Cambridge Crystallographic Data Centre, 12 Union Road, Cambridge CB2 1EZ, UK; fax: +44(0)1223-336033.

Disclosure statement

Conflict of interests: The authors declare that they have no conflict of interest.
Author contributions: All authors contributed equally to this work.
Ethical approval: All ethical guidelines have been adhered.
Sample availability: Samples of the compounds are available from the author.

ORCID

Praveen Singh
http://orcid.org/0000-0002-4740-3152
Ranjeet Kumar
http://orcid.org/0000-0003-1808-2473
Ashish Kumar Tewari
http://orcid.org/0000-0002-1388-5843

References

[1]. Breslin, H. J.; Cai, C.; Miskowski, T. A.; Coutlrho, S. V.; Zhang, S. P.; Pamela, H.; He, W. *Bioorg. Med. Chem. Lett.* **2006**, *16*, 2505-2508.
[2]. Yadav, M. R.; Puntambekar, D. S.; Sarathy, K. P.; Vengurlekar, S.; Giridhar, R. *Ind. J. Chem. B* **2005**, *45*, 475-482.
[3]. Matysiak, J.; Niewiadomy, A.; Niewiadomy, G. M.; Krajewska-kulak, E. *Farmaco* **2003**, *58*, 455-461.
[4]. Dahiya, R. *Sci. Pharm.* **2008**, *71*, 217-240.
[5]. Kapoor, V. K.; Dubey, S.; Mahindroo, N. *Ind. J. Chem. B* **2000**, *39*, 27-30.
[6]. Takakura, Y.; Kitajima, M.; Matsumoto, S.; Hashida, M.; Sezaki, H. *Int. J. Pharm.* **1987**, *37*, 135-143.
[7]. Khabnadideh, S.; Rezaei, Z.; khalafi-Nezhad, A.; Bahrinajafi, R.; Mohamadi, R.; Farrokhroz, A. A. *Bioorg. Med. Chem. Lett.* **2003**, *13*, 2863-2865.
[8]. Cheng, J.; Xie, J.; Luo, X. *Bioorg. Med. Chem. Lett.* **2005**, *15*, 267-269.
[9]. Narayanan, S.; Vangapandu, S.; Jain, R. *Bioorg. Med. Chem. Lett.* **2001**, *11*, 1133-1136.
[10]. Nair, S. C.; Panikkar, B.; Akamanchi, K. G.; Panikkar, K. R. *Cancer Lett.* **1991**, *60*, 253-258.
[11]. Nanidpour, L.; Shadnia, H.; Shafaroodi, H.; Amini, M.; Denpour, A. R.; Shafiee, A. *Bioorg. Med. Chem.* **2007**, *15*, 1976-1982.
[12]. Thomas, H. M.; Jonathan, B. R.; Emily, F. C. *Bioorg Med. Chem. Lett.* **2004**, *14*, 3721-3725.

[13]. Lee, J. C.; Laydon, J. T.; Mcdonnell, P. C.; Gallagher, T. F.; Kumar, S.; Green, D.; McNulty, D.; Blumanthal, M.; Heys, J. R.; Landvatles, S. W.; Strickler, J. E.; McLaughlin, M. M.; Siemens, J. R.; Fischer, S. M.; Livi, J. P.; While, J. R.; Adam, J. L.; Young, P. R. *Nature* **1994**, *372*, 739-746.
[14]. Maier, T.; Schmierer, R.; Bauer, K.; Bieringer, H.; Buerstell, H.; Sachre, B. *US Patent* 1989, 4820335.
[15]. Maier, T.; Schmierer, R.; Bauer, K.; Bieringer, H.; Buerstell, H.; Sachre, B. *Chem. Abstr.* 1989, 19494.
[16]. Schmierer, R.; Mildenberger, H.; Buerstell, H. *German Patent* 1987, 361464.
[17]. Schmierer, R.; Mildenberger, H.; Buerstell, H.; *Chem. Abstr*. 1988, 37838.
[18]. Cioli, V.; Putzolu, S.; Rossi, V.; Barcellona, P. S.; Corradino, C. *Toxicol. Appl. Pharmacol*. **1979**, *50*, 283-289.
[19]. Satoru I. *Japn Kokkai Tokyo Koho* JP 01, 117, 867, 1989; Chem. Abstr. 1989, 111, 214482.
[20]. Tayebee, R.; Ghadamgahi, M. *Am. J. Org. Chem.* **2012**, *2*, 25-27.
[21]. Kool, E. T. *Chem. Rev.* **1997**, *97*, 1473-1488.
[22]. Bugg, Introduction to Enzyme and Coenzyme Chemistry Blackwell Publishing Ltd, Oxford, UK, 2004.
[23]. Keskin, O.; Gursoy, A.; Ma, B.; Nussinov, R. *Chem. Rev.* **2008**, *108*, 1225-1244.
[24]. Sarker, S. D.; Nahar, L. Chemistry for Pharmacy Students: General, Organic and Natural Product Chemistry, John Wiley & Sons Ltd, London, England, 2007.
[25]. Baures, P. W.; Rush, J. R.; Wiznycia, A. V.; Desper, J.; Helfrich, B. A.; Beatty, A. M. *Cryst. Growth Des*. **2002**, *2*, 653-664.
[26]. Ugono, O.; Rath, N. P.; Beatty, A. M. *Cryst. Growth Des*. **2009**, *9*, 4595-4598.
[27]. Aakeroy, C. B.; Desper, J.; Urbina, J. F. *Chem. Comm.* **2005**, 2820-2822.
[28]. Aakeroy, C. B.; Desper, J.; Hussain, I. *Cryst. Growth Des*. **2006**, *6*, 474-374.
[29]. Nguyen, T. L.; Fowler, F. W.; Lauher, J. W. *J. Am. Chem. Soc*. **2001**, *123*, 11057-11064.
[30]. Prins, L. J.; Reinhoudt, D. N.; Timmerman, P. *Angew. Chem. Int. Ed*. **2001**, *40*, 2382-2426.
[31]. Desiraju, G. R. *Nature*, **2001**, *412*, 397-400.
[32]. Allen, F. H.; Motherwell, W. D. S.; Raithby, P. R.; Shields, G. P.; Taylor, R. *New. J. Chem.* **1999**, *23*, 25-34.
[33]. Sethuraman, V.; Stanley, N.; Muthiah, P. T.; Sheldrick, W. S.; Winter, M.; Luger, P.; Weber, M. *Cryst. Growth. Des.* **2003**, *3*, 823-8228.
[34]. Michal, A.; Jedrzej, M.; Kacper, W. R.; Andrzej, K. *Cryst. Growth Des*. **2015**, *15*, 1658-1665.
[35]. Damian, P.; Kamil, F. D.; Andrzej, K. *Cryst. Growth Des*. **2012**, *12*, 4302-4305.
[36]. Szafrannski, M.; Katrusiak, A.; McIntyre, G. J. *Phys. Rev. Lett.* **2002**, *89*, 5507-5510.
[37]. Katrusiak, A.; Szafranski, M. *J. Am. Chem. Soc*. **2006**, *128*, 15775-15785.
[38]. Wenbo, L.; Ann, M. *J. Magn. Reson.* **2012**, *222*, 74-80.
[39]. Witold, Z.; Andrzej, K. *Cryst. Growth Des.* **2013**, *13*, 696-700.
[40]. Christopher, J. S.; Paul, D. B. *Cryst. Growth Des*. **2013**, *13*, 2866-2871.
[41]. Desiraju, G. R. *Acc. Chem. Res.* **2002**, *35*, 565-573.
[42]. Steiner, T.; Desiraju, G. R. *Chem. Commun*. **1998**, 891-892.
[43]. Sheldrick, G. M. *ActaCrystallog. A* **2008**, *A64*, 112-122.
[44]. Farrugia, L. J. *J. Appl. Crystallog.* **1999**, *32*, 837-838.
[45]. Macrae, C. F.; Edgington, P. R.; McCabe, P.; Pidcock, E.; Shields, G. P.; Taylor, R.; Towler, M.; Van de Streek, J. *J. Appl. Cryst.* **2006**, 39, 453-457.
[46]. Spek, A. L. *Acta Crystallog. A* **1990**, *46*, C34.
[47]. McKinnon, J. J.; Spackman, M. A.; Mitchell, A. S. *Acta Crystallogr. B* **2004**, *60*, 627-668.
[48]. Ranjeet, K.; Pratima Y.; Shiv, P.; Krishnan R. K.; Balasubramanian, S.; Ashish K. T. *Chem. Select* **2017**, *2*, 3444-3451.
[49]. Tewari, A. K.; Srivastava, P.; Singh, V. P.; Singh, P.; Kumar, R.; Khanna, R. S.; Srivastava, P.; Gnanasekaran, R.; Hobza, P. *New J. Chem.* **2014**, *38*, 4885-4892.
[50]. Tewari, A. K.; Srivastava, P.; Puerta, C.; Valerga, P. *J. Mol. Struct.* **2009**, *921*, 251-254.
[51]. Tewari, A. K.; Srivastava, P.; Singh, V. P.; Puerta, C.; Pedro, V. *Arkivoc* **2010**, *9*, 127-136.
[52]. Dubey, R.; Tewari, A. K.; Ravikumar, K.; Sridhar, B. *J. Chem. Crystallogr.* **2011**, *41*, 886-890.
[53]. Luo, Y. H.; Chen-Guang, Z.; Bing, X.; Bai-W. S. *Cryst. Eng. Comm*. **2012**, *14*, 6860-6868.
[54]. Sohail, S.; Naghmana, R.; Shaaban, K. M. *Eur. J. Chem.* **2017**, *8(1)*, 15-17.
[55]. Akiko, O.; Toyokazu, M. S.; Genta, T.; Noriyuki, Y. *Eur. J. Chem.* **2017**, *8(1)*, 33-41.